THE JOURNAL OF BIOLOGICAL CHEMISTRY
Vol. 279, No. 8, Issue of February 20, pp. 6414–6425, 2004
Printed in U.S.A.

Transcriptional Profiling of *ubp10* Null Mutant Reveals Altered Subtelomeric Gene Expression and Insurgence of Oxidative Stress Response*

Received for publication, June 18, 2003, and in revised form, November 7, 2003
Published, JBC Papers in Press, November 17, 2003, DOI 10.1074/jbc.M306464200

Ivan Orlandi‡, Maurizio Bettiga, Lilia Alberghina, and Marina Vai§

From the Università degli Studi di Milano-Bicocca, Dipartimento di Biotecnologie e Bioscienze, Piazza della Scienza 2, 20126 Milano, Italy

***UBP10* codes for a deubiquitinating enzyme of *Saccharomyces cerevisiae* whose loss of function determines slow growth rate and partial impairment of silencing at telomeres and *HM* loci. A genome-wide analysis performed on a *ubp10* disruptant revealed alterations in expression of subtelomeric genes together with a broad change in the whole transcriptional profile, closely parallel to that induced by oxidative stress. This response was accompanied by intracellular accumulation of reactive oxygen species as well as by DNA fragmentation and phosphatidylserine externalization, two markers of apoptosis. *SIR4* inactivation mitigated the wide transcriptome remodeling of the *ubp10* null mutant affecting particularly the stress transcriptional profile. Moreover, the *ubp10sir4* disruptant did not display apoptotic markers. These results argue in favor of an involvement of deubiquitination in transcriptional control and suggest a linkage between oxidative stress and apoptotic pathway in budding yeast.**

Covalent attachment of ubiquitin (Ub)[1] to specific proteins represents a reversible post-translational modification associated not only with the removal of damaged or misfolded proteins but also involved in the regulation of different important cellular processes from signal transduction and cell cycle progression to endocytosis and apoptosis (1–5). The complexity of the Ub-dependent system reflects the wide range of its targets including cell cycle regulatory proteins like cyclins, oncogenes such as c-*mos*, c-*jun,* and c-*fos*, and tumor suppressor genes products such as p53. It is not surprising that perturbations in ubiquitination are implicated in the pathogenesis of several neoplastic and neurodegenerative diseases (6–8).

Important for the efficiency of the Ub-dependent pathway is the activity of a family of deubiquitinating enzymes (Dubs) acting as specific thiol proteases. These enzymes hydrolyze the linkage between the C-terminal Gly-76 of Ub and a Lys residue of a given substrate or of another Ub molecule. Dubs represent the largest known group of enzymes in the Ub system, and they fall into two distinct types: Ub C-terminal hydrolases and Ub-specific processing proteases (Ubps). The former includes low molecular weight enzymes releasing Ub from small size substrates such as peptides or glutathione; the latter includes higher molecular weight enzymes removing Ub from different substrates, at least *in vitro*. Ubps are highly divergent, but they contain several short consensus sequences (Cys and His boxes) essential for their enzymatic activity (1). Despite the identification of a great number of Dubs, their physiological roles remain quite obscure. They are required at several levels along the Ub pathway playing different functions. Ub is always synthesized as a precursor requiring removal of C-terminal peptides or amino acids; so Dubs are needed to generate Ub monomers. Furthermore, activated Ub can form stable complexes with abundant intracellular nucleophiles, such as amines and glutathione. This reaction, if not balanced, leads to a depletion of the cellular Ub pool. Moreover, after proteasome-dependent proteolysis of the substrate, released poly-Ub chains have to be rapidly disassembled. Finally, besides being involved in Ub recycling, Dubs play a regulatory function controlling ubiquitination level and activity of ubiquitinated proteins (9–11).

After the complete sequencing of the *Saccharomyces cerevisiae* genome, 17 genes encoding Dubs have been identified, among which are 16 Ubps. Few Ubps have a known physiological function (12). For example, Ubp14 disassembles unanchored polyubiquitin chains into monomeric Ub (13), and Ubp4/Doa4, similar to human oncogene *tre-2* (14), plays an important role in Ub recycling from both proteasome and vacuole (15–17). In yeast, the genetic redundancy of Ubps suggests a high degree of substrate specificity and thus a direct involvement in the activity of specific proteins, whereas the fact that none of the different Ubps is encoded by an essential gene points to some overlapping functions. We focused our studies on the *UBP10/DOT4* gene because of the intriguing *ubp10* phenotype. First, cells lacking Ubp10p show a partial loss of silencing at telomeres and at the mating type (*HM*) loci (18), a reduction in Sir4p level in agreement with a Ubp10p nuclear localization and with its ability to interact with Sir4p in a two-hybrid assay (19). Second, *ubp10* mutants display growth defects at different temperatures exacerbated when *UBP10* is inactivated in strains with several auxotrophic markers (12). The slow growth rate can be partially complemented by mutations in a subunit of the 26 S proteasome (*doa3-1*) or by deletions of *SIR2*, *SIR3,* or *SIR4* suggesting that Ubp10p activity is important for restricting silent information regulator (Sir) proteins to the normal silent loci by the regulation of Sir4p (19). In *S. cerevisiae* the products of the four *SIR* genes are important factors for the establishment and maintenance of a specialized chromatin

* This work was supported in part by grants from AIRC, 2002, and Progetto Strategico Terapia Preclinica in Oncologia, 2002 (to L. A.). The costs of publication of this article were defrayed in part by the payment of page charges. This article must therefore be hereby marked "*advertisement*" in accordance with 18 U.S.C. Section 1734 solely to indicate this fact.

‡ Recipient of a fellowship from Fondazione Levi-Montalcini.
§ To whom correspondence should be addressed. Tel.: 39-0264483531; Fax: 39-0264483565; E-mail: marina.vai@unimib.it.

[1] The abbreviations used are: Ub, ubiquitin; Dubs, deubiquitinating enzymes; Ubps, Ub-specific processing proteases; Sir, silent information regulator; ROS, reactive oxygen species; TUNEL, TdT-mediated dUTP nick end labeling; ORFs, open reading frames; RT, reverse transcription; FITC, fluorescein isothiocyanate.

structure, called silent chromatin, analogous to heterochromatin of higher eukaryotes. Silent chromatin is responsible for silencing at the *HM* loci, telomeres, and rDNA repeats. All the Sir proteins contribute to silencing the *HM* loci, whereas silencing at telomeres requires Sir2p, Sir3p, and Sir4p (reviewed in Refs. 20 and 21). In addition, Sir2p, an NAD^+-dependent deacetylase, is involved in rDNA silencing (reviewed in Ref. 22). Sir proteins are recruited to DNA through a network of protein-protein interactions involving Sir proteins themselves and other factors including Rap1, Abf1, the origin recognition complex, and histones H3 and H4. The silencing efficiency is linked to the relative concentration of Sir proteins due to competition among the different silent loci for limited Sir proteins. In this regard, deletion of *SIR4* severely reduces telomeric and *HM* silencing, preventing Sir3p recruitment to the telomeres (23), and enhances rDNA silencing indicating that telomeres and rDNA repeats compete for a limited amount of Sir2p (24). Conversely, *SIR4* overexpression disrupts silencing suggesting that Sir4p overexpression may titrate Sir3p away from chromatin and Sir2p from the rDNA (25). In fact, Sir4p is a large multidomain protein that is able to interact with many other proteins such as Sir2p, Sir3p, Sir4p, Rap1p, and yKu70p (20, 26). In particular Sir4p binding to Rap1p initiates the sequential assembly of the Sir complex at telomeric ends allowing the subsequent spreading along the chromosome (27). Moreover, it has also been reported that the C-terminal domain of Sir4p can associate with Ubp3p (28) and Ubp10p (19), suggesting that ubiquitination could target other proteins of the silencing machinery in addition to histones.

However, the failure in detecting ubiquitinated Sir4p (19) together with the partial complementation of the *ubp10* growth defect observed by inhibition of endocytosis (29) suggest that precise functions and additional targets of Ubp10p remain to be discovered.

In this report we integrated a genome-wide approach with phenotypic analyses to dissect mechanisms underlying Ubp10p function. Because Ub is involved in many physiological processes and the *ubp10* phenotype indicates perturbations in different cellular functions, we thought that a global transcriptional profiling could be useful for extracting functional information to be verified by *in vivo* assays. Our analysis revealed that deletion of *UBP10* induced a huge transcriptome remodeling characterized by a reduced subtelomeric repression and up-regulation of stress-responsive genes. This was accompanied by accumulation of reactive oxygen species (ROS) and by appearance of apoptosis-like phenotypical markers. Following *SIR4* inactivation, these features were completely abrogated except for transcriptional derepression of silencing that partly reflects *SIR4* loss of function. These results further support that the Sir-mediated activity is influenced by (de)ubiquitin-dependent signaling mechanisms, and it is the first indication that in yeast a deubiquitinating enzyme may be involved in programmed cell death.

EXPERIMENTAL PROCEDURES

Strains and Growth Conditions—The *S. cerevisiae* haploid strains *ubp10*Δ (*UBP10*::*HIS3*), *sir4*Δ (*SIR4*::*LEU2*), and *ubp10*Δ*sir4*Δ (*UBP10*::*HIS3, SIR4*::*LEU2*) were generated from the wild type strain W303-1A (*MAT***a** *ade2-1 his3-11,15 trp1-1 ura3-1 leu2-3,112 can1-100*) and from the same strain but of opposite mating type (W303-1B) by one-step gene disruption (30). *UBP10* inactivation was also carried out in an other strain, BY4741 (*MATa his3Δ1 leu2Δ0 met15Δ0 ura3Δ0*), from Euroscarf. Yeast cells were grown in batches at 30 °C in Difco yeast nitrogen base medium without amino acids (YNB−aa; 6.7 g/liter) containing 2% glucose and the required supplements. Growth on non-fermentative carbon source was carried out on 2% glycerol, 0.5% peptone, YNB−aa, and the required supplements. Cell number and percentage of budded cells were determined as described previously (31).

Recombinant DNA Procedures and Plasmids—Standard protocols were used for recombinant DNA manipulation and yeast transformation (32, 33). Full-length *UBP10* and *SIR4* genes were amplified from yeast chromosomal DNA with the following primers: UBP10-up (5′-CAGAGTCAGAGTGGCGCACTA-3′) and UBP10-down (5′-CGCATTGGGCTCCAAGGGTAT-3′), SIR4-up (5′-ACCGGTATCTGGGCTGGTGTTGA-3′) and SIR4-down (5′-CATCCCTGCAGCTGTCCGAACAA-3′). The two PCR products, containing the *UBP10* coding sequence flanked by 561 bases upstream and 718 bases downstream and *SIR4*, spanning between −523 and 5071 nucleotides from the ATG, were subcloned into the pCR®-Blunt vector (Invitrogen) to produce pUBP10 and pSIR4 plasmids, respectively. PCR products were routinely checked by sequence analysis. To generate *ubp10*::*HIS3* cassette, a BamHI/XhoI fragment containing the *HIS3* gene was inserted by blunt-end ligation into pUBP10 cut with ClaI and HpaI. Blunt-end cloning of a 2.2-kb SalI/XhoI *LEU2* fragment into ScaI/ClaI-digested pSIR4 replaces the *SIR4* ORF. Gene disruptions were confirmed by diagnostic PCR and Southern analyses.

Gene Chip® Analysis—Cells for RNA isolation were rapidly collected by filtration, and filters were frozen at −80 °C. Total RNA was extracted from frozen cells according to the method of selective precipitation with LiCl (34). Fragmented antisense cRNA was prepared following Affymetrix (Santa Clara, CA) recommendations. Briefly, double-stranded cDNA was retro-transcribed from 30 μg of total RNA using a modified oligo(dT) primer with a 5′ T7 RNA polymerase promoter sequence and the Superscript Choice System for cDNA synthesis (Invitrogen). cRNA, obtained using an ENZO kit (Affymetrix), was purified on an affinity column (RNeasy, Qiagen). Analysis was done by hybridizing the fragmented cRNAs to the Affymetrix GeneChip® Yeast Genome S98 array, which permits the monitoring of the mRNA abundance from 6400 ORFs. Probe array hybridizations were carried out under rotation at 45 °C for 16 h as described (35). The arrays, stained by incubation with 2 μg/ml phycoerythrin-streptavidin (Molecular Probes, Eugene, OR) and 1 mg/ml acetylated bovine serum albumin (Sigma), were read at a resolution of 7.5 μm by a confocal scanner and analyzed with the MicroArray Suite 4.0 Gene Expression analysis program (both from Affymetrix). The whole set of data is available at www.ncbi.nlm.nih.gov/geo/(GEO series accession number GSE804).

Reverse Transcription (RT)-PCR—Total RNA, prepared as described above for Gene Chip analysis, was purified using the RNeasy RNA purification kit and then treated with DNase I, RNase-free (Roche Applied Science), for 1 h at 37 °C followed by phenol extraction and ethanol precipitation. RT-PCR was carried out to amplify the *ARO9*, *AUT4*, *CTT1*, *GLK1*, *GPD1*, *HSP26*, *HXK1*, and *ACT1* mRNAs using the Access RT-PCR System (Promega) following the manufacturer's instructions. The number of cycles was lowered to 15/20 so that amplification was in the exponential range. Experiments were repeated at least twice with different RNA preparations. Primers sequences used for PCRs are available upon request.

Northern Analysis—Northern analysis was performed as reported previously, using ^{32}P-radiolabeled RNA probes generated by *in vitro* transcription (36). *ACT1* mRNA was used as an internal standard.

Test for Apoptotic Markers—Free intracellular radicals were detected with dihydrorhodamine 123 or dichlorodihydrofluorescein diacetate (dichlorofluorescein diacetate; Sigma) as described previously (37). For flow cytometric analysis, cells were incubated with dichlorofluorescein diacetate for 2 h and analyzed using a FACS® Star (BD Biosciences) with excitation and emission settings of 488 and 525–550 nm (filter FL1), respectively. TdT-mediated dUTP nick end labeling (TUNEL) test was performed according to Ref. 37, except for spheroplast preparations carried out with Zymolase 100T (ICN Biomedicals). DNA ends were labeled using the *In Situ* Cell Death Detection Kit, POD (Roche Applied Science). Cells were examined under light microscope and through a fluorescein optical filter. Externalization of phosphatidylserine was detected essentially as described (38). Spheroplasts were examined under fluorescence microscope after 20 min of incubation at room temperature with FITC-labeled annexin V (ApoAlert Annexin V Apoptosis Kit; Clontech, Palo Alto, CA) and propidium iodide (50 μg/ml).

RESULTS AND DISCUSSION

Transcriptome Profiling of ubp10 Null Mutant Reveals a Cellular Stress Response—ubp10 mutants have a detectable phenotype characterized by an impairment of silencing at telomeres and *HM* loci and a reduced growth partially complemented by *SIR4* inactivation (12, 18, 19). We generated a set of null mutants carrying single or double disruptions (*ubp10*, *sir4*, *ubp10 sir4*) in the wild type backgrounds W303-1A (mating

TABLE I

Group of 82 stress-related genes that display differential (increased) expression between ubp10Δ and W303–1A strains

Genes are divided into 11 functional sub-groups St, genes containing in the promoter region one or more stress-responsive elements (STRE); Et, genes whose expression usually increased after a treatment with high ethanol concentrations; H_2O_2, genes whose expression usually increased upon hydrogen peroxide stimulus; Os, genes whose expression usually increased in hyperosmotic stress conditions.

Gene name	ORF code	Fold change	Gene description	Notes
I-SUGAR METABOLISM				
HXK1	YFR053C	44.3	Esokinase I	St,Et
GLK1	YCL040W	8.3	Glucokinase	St,Et,H_2O_2,Os
HXT4	YHR092C	4.9	High-affinity glucose transporter	St
HXT6	YDR343C	4.1	Hexose transporter	St
HXT7	YDR342C	3.7	Hexose transporter	St
YDR516C		3.3	73% identical to Glk1p	Et,Os
YLR345W		3.7	Protein with similarity to fructose-2,6-bisphosphatase	Os
II-TREHALOSE, GLYCEROL, GLYCOGEN METABOLISM				
GPD1	YDL022W	4.3	Glycerol 3-phosphate dehydrogenase	Et,H_2O_2,Os
GPM2	YDL021W	4.9	Phosphoglycerate mutase	Et
GPP2	YER062C	2.7	Glycerol-1-phosphatase	Et,H_2O_2,Os
ATH1	YPR026W	5.1	α,α-trehalase	Et,Os
NTH1	YDR001C	2.6	Neutral trehalase (α,α-trehalase)	St,Et
NTH2	YBR001C	2.3	Neutral trehalase, highly homologous to Nth1p	Et,Os
TPS1	YBR126C	2.1	56 kD synthase subunit of trehalose-6-phosphate synthase\phosphatase complex	St,Et,H_2O_2,Os
TPS2	YDR074W	5.3	α,α-trehalose-phosphate synthase 102 Kda subunit	St,Et,Os
TSL1	YML100W	8.0	α,α-trehalose-phosphate synthase 123 Kda subunit	St,Et,Os
GLC3	YEL011W	8.1	Glucanosyltransferase	Et,Os
GSY1	YFR015C	10.6	UDP-Glucose glucosyltransferase	Et,Os
GSY2	YLR258W	3.7	Glycogen synthase	St,Os
PGM2	YMR105C	4.1	Phosphoglucomutase, major isoform	St,Et,H_2O_2,Os
GPH1	YPR160W	27.7	Glycogen phosphorylase	St,Os
GLG1	YKR058W	2.9	Self-glucosylating initiator of glycogen synthesis; similar to mammalian glycogenin	Et
III-PROTEINS WITH ANTIOXIDANT SCAVENGING/DEFENSE PROPERTIES				
GPX1	YKL026C	5.7	Glutathione peroxidase	H_2O_2
GRX1	YCL035C	2.2	Putative glutaredoxin (thiol-transferase)	Os
SOD2	YHR008C	2.5	Mn superoxide dismutase	H_2O_2
CCP1	YKR066C	2.1	Cytochrome-c peroxidase	H_2O_2
CTT1	YGR088W	6.7	Cytoplasmic catalase T	St,Et,H_2O_2
DAK1	YML070W	2.5	Putative dihydroxyacetone kinase	Et, H_2O_2
GTT1	YIR038C	3,6	Glutathione transferase	H_2O_2,Os
YBL064C		2.3	Putative peroxidase of the 1-Cys family	Os
YDR453C		5.6	Strong similarity to thiol-specific antioxidant proteins	H_2O_2,Os
IV-REDOX METABOLISM AND MITOCHONDRIAL FUNCTIONS				
CYC7	YEL039C	8.5	Iso-2-cytochrome c	St,Os
GRE2	YOL151W	2.4	Induced by osmotic stress\similar to dihydroflavonol 4-reductase from plant	Os
GRE3	YHR104W	3.8	Aldo-keto reductase	Et,Os
STF2	YGR008C	9.4	ATPase stabilizing factor; energy metabolism	Et,Os
YLR327C		34.9	Protein with similarity to ATPase stabilising factor Stf2p, expression depends on Msn2p in acidic stress conditions	Os
ALD2	YMR170C	3.9	Aldehyde dehydrogenase, (NAD(P)+), likely cytosolic	Et
ALD3	YMR169C	10.9	Aldehyde dehydrogenase (NAD(P)+)	Os
ALD4	YOR374W	2.9	Aldehyde dehydrogenase (E.C. 1.2.1.5)	Et
CYB2	YML054C	9.5	Cytochrome b2 [L-lactate cytochrome-c oxidoreductase]	Os
MDH2	YOL126C	3.1	Cytosolic malate dehydrogenase	St

TABLE I—*continued*

Gene name	ORF code	Fold change	Gene description	Notes
V-HEAT SHOCK PROTEINS				
HSP104	YLL026W	4.9		St,Et,H_2O_2,Os
HSP12	YFL014W	4.0		St,Et,H_2O_2,Os
HSP26	YBR072W	27.2		St,Et,H_2O_2,Os
HSP42	YDR171W	25.0	Sim. HSP26	Et,H_2O_2,Os
HSP78	YDR258C	2.6		Et,H_2O_2
HSP82	YPL240C	3.0		Et, H_2O_2
SSA4	YER103W	28.0	Hsp70	St,H_2O_2,Os
SSE2	YBR169C	10.7	Hsp70	Os
YRO1	YCR021C	239.7	Hsp30	St,Et,Os
YRO2	YBR054W	36.7	Hsp30	St,Et,Os
DDR48	YMR173W	2.2	Stress induced protein of unknown function	H_2O_2,Os
VI-AMINO ACID METABOLISM				
ARO10	YDR380W	78.6	Similar to pyruvate decarboxylase. Expression is correlated to YLR327C	Os
ARO9	YHR137W	36.5	Aromatic aminoacid aminotransferase II	Os
YHR087W		40.0	Depends on Msn2p in acidic stress conditions	Os
YLR327C		34.9	Depends on Msn2p in acidic stress conditions. Related to ARO10	Os
VII-SIGNAL TRANSDUCTION AND CONTROL OF GENE EXPRESSION				
TPK1	YJL164C	2.5	PKA catalytic subunit	St,Os
YAK1	YJL141C	3.6	Ser/Thr Kinase	St,Os
SSK1	YLR006C	2.1	Osmosensitive MAP kinase regulator	Os
YIL113W		6.3	Strong similarity to dual-specificity phosphatase Msg5p	St
YAP4	YOR028C	2.5	bZIP protein, can activate transcription from a promoter containing a Yap recognition site	Os
MGA1	YGR249W	33.8	Similar to heat shock transcription factor	
MSN1	YOL116W	2.8	Alias FUP1, HRB382, MSS10, PHD2. Multicopy suppressor of snf1	Os
PTK2	YJR059W	2.9	Putative serine\threonine protein kinase that enhances spermine uptake	H_2O_2,Os
TFS1	YLR178C	5.4	Nutrient-dependent cell cycle regulator, suppressor of cdc25 mutation	Os
YMR291W		6.8	Ser/Thr Kinase	Os
GIP2	YER054C	2.6	Glc7-interacting protein; shares homology with PIG2; contains conserved 25 residue motif, called the GVNK motif, also found in GAC1, PIG1, PIG2, and RGI, the mammalian type 1 phosphatase targeting subunit	Et
GSP2	YOR185C	3.2	GTP-binding protein involved in trafficking through nuclear pores	Os
GAC1	YOR178C	4.5	Protein phosphatase 1. Regulates Glc7p	St
VIII-CELL SURFACE				
CWP1	YKL096W	2.1	Cell wall mannoprotein	Os
SPI1	YER150W	33.8	Strong similarity to putative cell surface glycoprotein Sed1	Os
YGP1	YNL160W	10.3	Response to nutrient limitation. Homologous to SPS100	Et,Os
IX-PROTEOLYSIS				
SON1	YDL020C	2.2	Subunit of the regulatory particle of the proteasome	Et
UBI4	YLL039C	3.1	Ubiquitin	H_2O_2
LAP4	YKL103C	2.3	Vacuolar aminopeptidase	
PAI3	YMR174C	2.7	Cytoplasmic inhibitor of proteinase Pep4	Os
PRB1	YEL060C	2.3	Vacuolar protease B	Os
X-PROTEIN-VACUOLAR TARGETING AND AUTOPHAGY				
APG7	YHR171W	2.2	Autophagy	H_2O_2
AUT4	YCL038C	11.8	Membrane transporter	Et,H_2O_2
AUT7	YBL078C	5.6	Form a protein complex with Aut2p, to mediate attachment of autophagosomes to microtubules.	Et
XI-LIPID METABOLISM				
CKI1	YLR133W	2.7	Choline kinase	Os
ACH1	YBL015W	2.6	ACoA hydrolase	

TABLE II
Group of 24 subtelomeric genes, which display differential expression between upb10Δ and W303-1A strains

Gene name	ORF code	Fold change	Gene description
COS8	YHL048W	2.8	Unknown function
DAN3	YBR301W	2.2	Unknown function
DIA1	YMR316C	8.7	Unknown function
DLD3	YEL071W	-2.8	D-lactate dehydrogenase
LYS1	YIR034C	-2.5	Saccharopine dehydrogenase
MAL11	YGR289C	3.5	Alpha-glucoside transporter
MNT2	YGL257C	-2.7	Mannosyltransferase
MSC1	YML128C	4.4	C-terminal part starting with aa 262 causes growth inhibition when overexpressed
PAU6	YNR076W	2.1	Member of the seripauperin protein\gene
SEO1	YAL067C	-3.5	Suppressor of Sulfoxide Ethionine resistance
SUL1	YBR294W	-3.3	Putative sulfate permease
YBL109W		2.3	Unknown function
YDR542W		2.9	Unknown function
YEL074W		-2.3	Unknown function
YER188W		4.7	Unknown function
YHL046C		2.3	Unknown function
YHR218W		2.1	Gene in Y' repeat region
YIR044C		2.3	Unknown function
YLL067C		3.1	Unknown function
YMR316W		10.9	Unknown function
YPS5	YGL259W	2.4	Aspartic endopeptidase
YPS6	YIR039C	2.9	GPI-anchored aspartic protease
YRF1-5	YLR467W	3.6	Unknown function
YRF1-6	YNL339C	2.4	Unknown function

type a) and -1B (mating type α) whose phenotypes were similar to published ones (12, 19, 39).

To get insight into the cellular functions affected by *UBP10* inactivation, we first carried out a microarray analysis of the differential genome-wide expression profile of a *ubp10* mutant *versus* its isogenic wild type strain (W303-1A). Data from two independent pairs of experiments were analyzed. Cultures were harvested at a cellular density of 5×10^6/ml in exponential growth phase on 2% glucose/YNB medium, a growth condition in which the *ubp10* mutant showed a more severe phenotype. Transcript levels obtained from the two different strains were compared using the Affymetrix method of scaling. Reliability of the gene chip analysis was also evaluated by comparing transcript levels of three reference genes, *ACT1*, *PDA1,* and *HHO1*, commonly used as standards (40).

Comparison between *ubp10* null mutant and wild type strain revealed changes in transcript levels of a large fraction of the genome. Such remodeling of the transcriptome reflects perturbations of different cellular functions, and it can correlate with some phenotypic traits of *ubp10* cells, in particular with its involvement in telomeric silencing and with the requirement of Sir4p in maintaining proper chromatin function. Given the amount of information generated, only some relevant aspects will be presented in this report; the full data set is available at www.ncbi.nlm.nih.gov/geo/. Initially, genes with a known cellular role were clustered according to their physiological pathway. Both induced and repressed genes belonged to very heterogeneous functional categories; however, we found some classes to be more represented than others. The down-regulated group included genes coding for the following: (i) various transporters, such as tyrosine, glutamate, isoleucine permease, ammonium permease, biotin, and peptides carriers; (ii) ribosomal proteins and translational factors; and (iii) enzymes involved in the biosynthesis of arginine, lysine, tryptophan, and nucleotides. The down-regulation of some of these mRNAs could indicate an impairment in protein synthesis and nutrient transport related to the *ubp10* disruptant growth defect that is particularly evident when the deletion is made in strains with auxotrophic markers (especially *his3*, *leu2*, *lys2,* and *trp1*) (19). No change was observed in *GAP1* transcript in agreement with Northern analysis (29).

Among the genes whose expression was increased, a conspicuous group encoded the following: (i) enzymes involved in carbohydrate transport, metabolism, and energy generation; (ii) heat shock proteins; and (iii) transcription factors, such as Hap2, Hap4, Rox1, Yap4. Because many of these have been found previously to be down- or up-regulated in specific physiological conditions, we analyzed our results not only according to metabolic pathways but also on the basis of published data (41–44). This further clustering revealed that many of the genes induced in the *ubp10* null mutant had been proposed previously to offer cell protection in response to stress, *i.e.*

hyperosmotic or oxidative stress, heat shock, ethanol exposure, and starvation. These genes are listed in Table I depending on functional categories. In addition, we found a subset of 25 genes that were characterized by the presence of stress-responsive consensus sequences in their promoter regions. Transcription driven by stress-responsive elements through Msn2 and Msn4 factors has been demonstrated to be induced by a variety of stress conditions activating the general stress response (44). Among the 25 genes there was some coding for enzymes that synthesize trehalose (*TPS1*, *TPS2*, and *TSL1*), glycogen (*GSY1*, *GSY2*), and their precursors, as well as others encoding enzymes involved in the degradation of carbohydrates (*ATH1*, *NTH1*, *NTH2*, and *GPH1*). The simultaneous induction of both synthetic and catabolic enzymes allows cells to rapidly buffer and manage osmotic instability and energy reserves. In particular, trehalose protects cellular components from detrimental effects of stress by providing the energy required for renaturation of cellular structures and protecting cells and membranes from denaturation (42, 43, 45). Other genes involved in carbohydrate metabolism were *GPD1* and *GPP2* encoding glycerol-3-phosphate dehydrogenase and glycerol-1-phosphatase, respectively, two glycerol-producing enzymes that play a critical role in response to the hyperosmotic shock allowing the accumulation of glycerol as compatible osmolite (46).

Nine genes (*HSP26*, *HSP42*, *HSP78*, *HSP104*, *HSP12*, *YRO1, YRO2, SSE2*, and *SSA4*) encoding heat shock proteins were strongly up-regulated (Table I). Hsp104 is a member of the highly conserved Hsp100/Clp family and acts as a chaperone to disaggregate damaged proteins. *SSA4* encodes the cytosolic Hsp70 that prevents protein aggregation directly, and it is required for protein refolding together with Hsp40 and Hsp104. In addition, among the functions related to the metabolism of damaged proteins, in *ubp10* null mutant cells we found an induction of the polyubiquitin gene *UBI4* whose expression is normally enhanced under conditions of heat shock, starvation, respiratory growth or other conditions where damaged or partially denatured proteins need to be degraded to prevent their accumulation as aggregates (47). A vacuole-mediated process

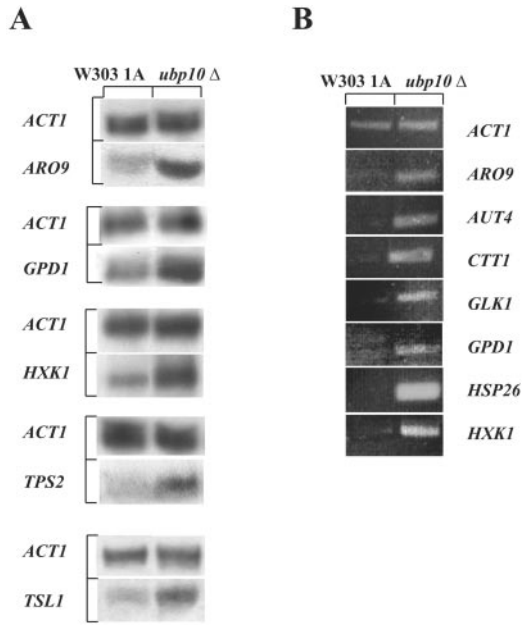

FIG. 1. **Validation of microarray data.** *A*, Northern analysis was performed on total RNA isolated from the *ubp10*Δ mutant and its isogenic wild type. About the same amount of RNA was loaded on each lane (20 μg) and hybridized with probes specific for the indicated genes. *ACT1* mRNA is shown as the loading control for each hybridization. *B*, the expression of *ARO9*, *AUT4*, *CTT1*, *GLK1*, *GPD1*, *HSP26,* and *HXK1* in the wild type (W303-1A) and *ubp10*Δ strains was analyzed by semi-quantitative RT-PCR as described under "Experimental Procedures." *ACT1* was used as a control. Similar data were obtained for RNA independent samples.

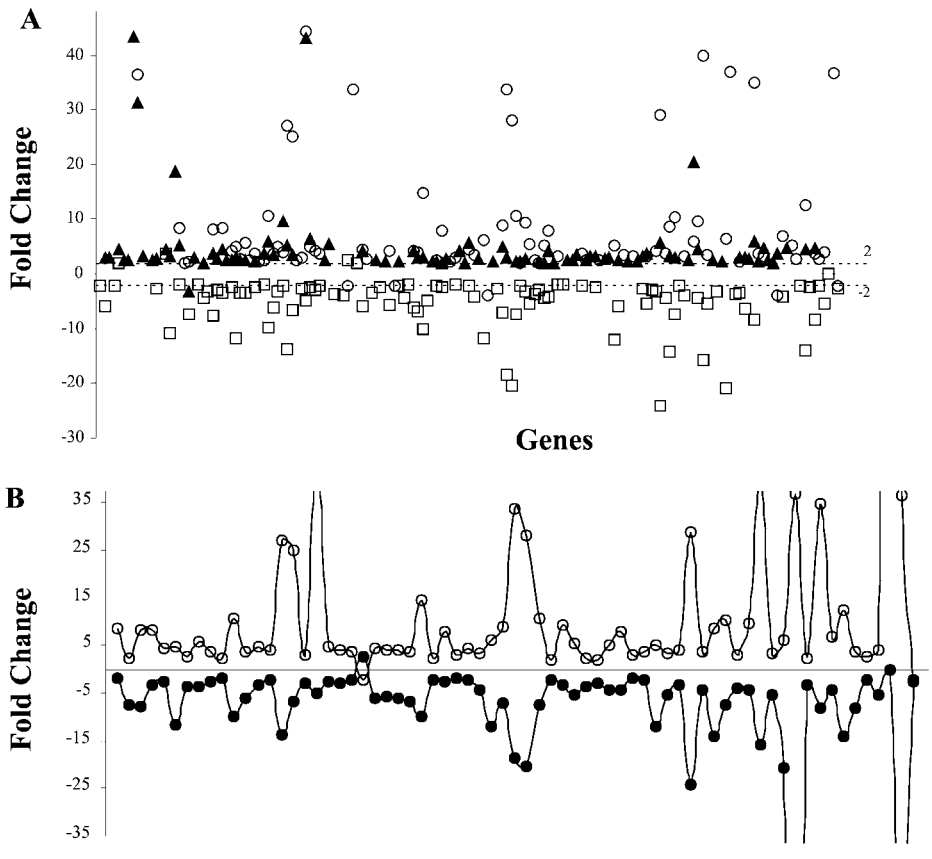

FIG. 2. ***SIR4* disruption suppresses the induction of the stress-related genes in the *ubp10*Δ mutant.** *A*, fold change values plot referred to a group of 156 stress-related genes, which display differential expression between *ubp10*Δ *versus* W303-1A (○), *ubp10*Δ*sir* 4 Δ *versus* W303-1A (▲), and *ubp10*Δ*sir4*Δ *versus ubp10*Δ (□). Values referred to *ARO10*, *YJL144W*, *YRO1*, and *YRO2* genes were omitted for a graphical reason. *B*, fold change values plot referred to a subgroup of 69 stress-related genes, which display differential expression between *ubp10*Δ *versus* W303-1A (○) and *ubp10*Δ*sir4*Δ *versus ubp10*Δ (●). Values referred to *YRO1*, *YRO2*, and *YJL144W* genes were omitted for the same reason as in *A*. Only genes with a fold change ≥|2| are shown.

TABLE III
Group of 54 subtelomeric genes, which display differential expression between ubp10Δsir4Δ and W303-1A strains

Gene name	ORF code	Fold change	Gene description
AAD4	YDL243C	2.4	Hypothetical aryl-alcohol dehydrogenase
AAD14	YNL331C	2.9	Hypothetical aryl-alcohol dehydrogenase
AYT1	YLL063C	2.1	Transacetylase
CHA1	YCL064C	4.5	Catabolic serine (threonine) dehydratase
COS2	YBR302C	2.1	Protein coded from subtelomeric region
C0S3	YML132W	2.5	Protein with similarity to subtelomerically-encoded proteins
COS5	YJR161C	2.2	Protein with similarity to members of the Ybr302p\/Ycr007p\/Cos8p\/Cos9p family, encoded from subtelomeric region
COS8	YHL048W	2.5	Protein with similarity to subtelomerically-encoded proteins
COS9	YKL219W	2.1	Protein with similarity to subtelomerically-encoded proteins
COX14	YML129C	2.2	mitochondrial membrane protein
FRE2	YKL220C	4.4	Ferric reductase, similar to Fre1p
HXK1	YFR053C	43.1	Hexokinase I (also called Hexokinase A)
HXT9	YJL219W	2.5	High-affinity hexose transporter
MAL11	YGR289C	5.0	Alpha-glucoside transporter
MAL31	YBR298C	3.7	Maltose permease
MAL33	YBR297W	2.7	Maltose fermentation regulatory protein
MHT1	YLL062C	2.4	Weak similarity to *M.leprae* metH2 protein
MSC1	YML128C	4.1	Meiotic Sister-Chromatid recombination protein
PAU3	YCR104W	2.6	Member of the seripauperin protein\gene family
PAU4	YLR461W	2.9	Member of the seripauperin protein\gene family
YAL068C		48.3	Strong similarity to subtelomerically-encoded proteins
YAL069W		4.8	Hypothetical protein
YAR060C		2.2	Strong similarity to hypothetical protein YHR212C
YAR061W		2.6	Putative pseudogene
YBL112C		-2.7	Strong similarity to subtelomerically-encoded proteins
YCL074W		9.3	Reverse transcriptase
YDL247W		3.3	Strong similarity to sugar transport proteins
YEL073C		6.8	Similarity to YJR108W
YEL074W		14.2	Similarity to subtelomerically-encoded proteins
YER186C		2.4	Weak similarity to hypothetical protein YMR316W
YER187W		3.4	Similarity to killer toxin KHS precursor
YER188W		5.5	Hypothetical protein
YFL063W		4.9	Strong similarity to subtelomerically-encoded proteins
YFR057W		4.3	Weak similarity to Cha4p
YGL261C		2.1	Strong similarity to members of the Srp1/Tip1 family
YGR294W		2.2	Strong similarity to members of the Srp1p/Tip1p family
YHL044W		2.5	Similarity to subtelomerically-encoded proteins
YHL050C		-5.8	Strong similarity to subtelomerically-encoded proteins
YIR043C		5.0	Putative pseudogene
YJR160C		3.8	Strong similarity to Mal31p
YJR162C		5.5	Strong similarity to subtelomerically-encoded proteins
YKL225W		3.2	Strong similarity to Gin11p, YKL225W and other subtelomerically-encoded proteins

TABLE III—*continued*

Gene name	ORF code	Fold change	Gene description
YKR104W		2.5	Similarity to multidrug resistance proteins
YLL065W		3.3	Growth inhibitory protein
YLR462W		2.1	Strong similarity to subtelomerically-encoded proteins
YMR316W		2.6	similarity to YOR385w and YNL165w
YMR320W		2.5	Hypothetical protein
YMR322C		4.7	strong similarity to YPL280w, YOR391c and YDR533c
YNL335W		11.1	Similarity to M.verrucaria cyanamide hydratase
YNL337W		5.2	Strong similarity to subtelomeric encoded proteins
YNR077C		3.9	Strong similarity to subtelomeric encoded proteins
YOR394W		3.1	Strong similarity to members of the Srp1p/Tip1p family
YRF1-5	YLR467W	-2.8	Strong similarity to subtelomerically-encoded proteins
YRF1-6	YNL339C	-2.5	Strong similarity to subtelomerically-encoded proteins

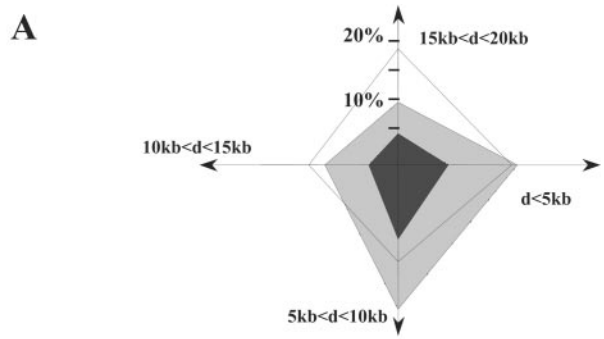

B

	HMLALPHA1	*HMLALPHA2*	*HMRA1*	*HMRA2*
ubp10Δ	*NC*	*2.4*	*3.2*	*NC*
sir4Δ	*NC*	*4.8*	*6.1*	*4.3*
ubp10Δ sir4Δ	*NC*	*4.8*	*6.3*	*2.9*

FIG. 3. ***UBP10* inactivation influences genes near telomeric ends.** *A*, the diagram indicates how the fraction of derepressed genes varied with distance from the telomere, outlining a peculiar quadrilateral shape (kite plot) for each mutant. Each semi-axis represents a specific region as indicated (*d*, distance from the telomere). *ubp10Δ* (*dark gray*), *sir4Δ* (*light gray*), and *ubp10Δsir4Δ* (*white*). *B*, reduced silencing at the *HM* loci. Fold change values are reported. *NC*, not changed.

called autophagy also contributes in the removing of damaged cellular components (48); *UBP10* loss of function induced the expression of genes involved in this process (*APG7*, *AUT4,* and *AUT7*) (Table I).

Changes in the expression of components of the Ub system have been shown to take place in response to oxidative stress (49, 50); a notable feature of the *ubp10* mutant transcriptome was the induction of genes whose products act as scavengers in the enzymatic defense against oxidizing agents that potentially damage proteins and nucleic acids (51, 52). We detected *GRX1*, encoding the cytoplasmic glutaredoxin; *GPX1*, glutathione peroxidase; *SOD2*, mitochondrial Mn-superoxide dismutase; *CCP1*, mitochondrial cytochrome *c* peroxidase, *CTT1*, cytoplasmic catalase T; and *GTT1*, glutathione transferase. In particular, the increased expression of *SOD2*, *CCP1*, and *CTT1* is a typical phenomenon observed during respiratory metabolism to counteract ROS production (52–54).

To confirm the reliability of the microarray data, a subset of selected genes, belonging to different functional groups that exhibited small and large transcriptional changes, was further characterized by Northern analysis (Fig. 1*A*) and semiquantitative RT-PCR (Fig. 1*B*). As illustrated in Fig. 1, the results obtained with the two different approaches revealed the same pattern of induction for the nine genes analyzed as that shown by microarray analysis (Table I).

In conclusion, the lack of Ubp10p activity results in the activation of a defined program of gene expression that displays all the characteristics of an adaptive response induced by oxidative stress. In *ubp10* mutants as in oxidatively stressed cells, there is an increased need for protection against a damage in cellular homeostasis that takes place without external perturbation but only upon the absence of a deubiquitinating activity.

SIR4 Inactivation Suppresses the Transcriptional Stress Response of the ubp10 Mutant—As a further refinement of our

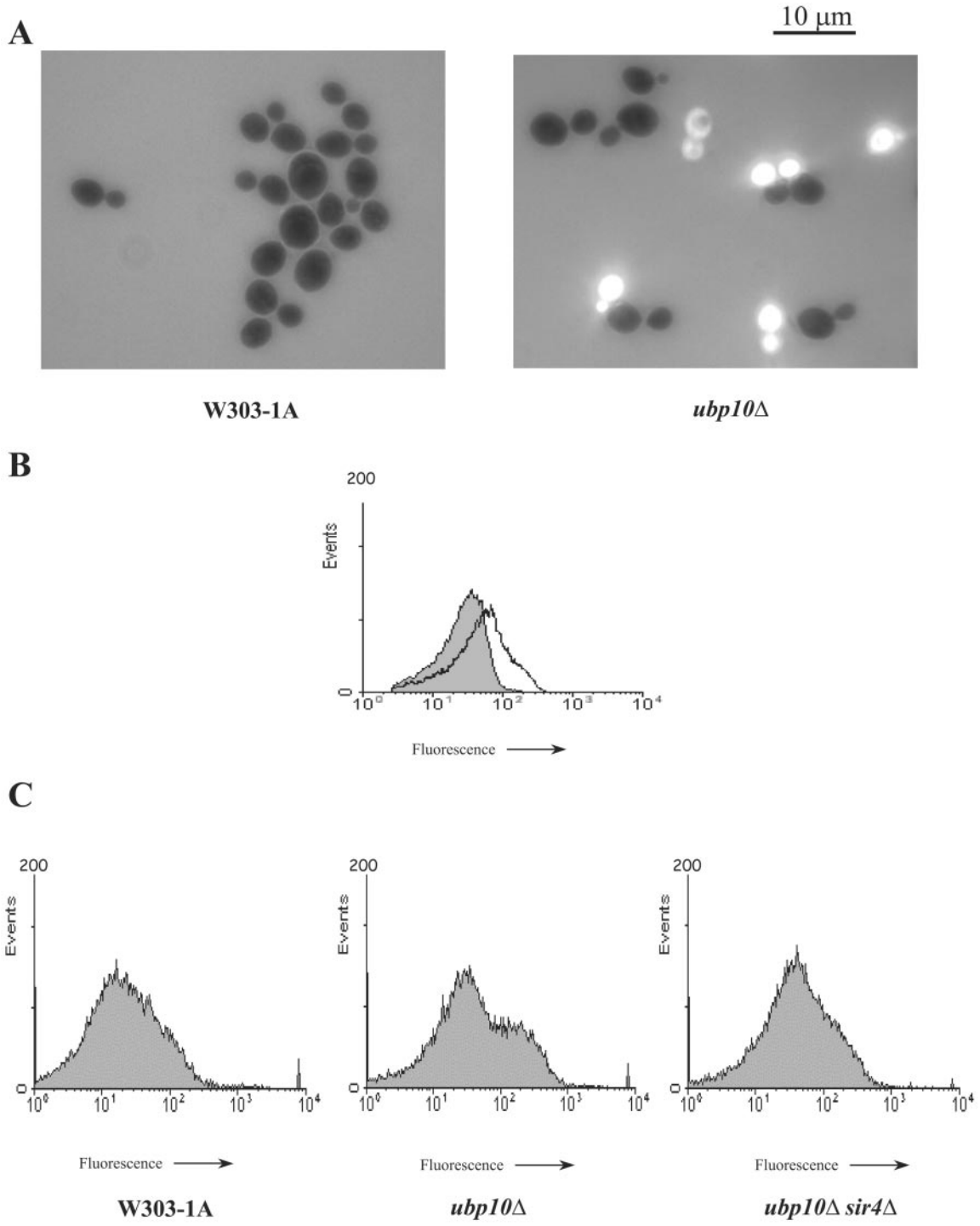

FIG. 4. ***ubp10*Δ mutant cells accumulate ROS.** *A*, fluorescence microscopy image of W303-1A and *ubp10*Δ cells growing on 2% glucose (fermentable carbon source). Cells stained *in vivo* with the ROS-specific dye dichlorodihydrofluorescein diacetate for 2 h. *B*, flow cytometric analysis of ROS content in BY4741 (*gray*) and *ubp10*Δ (*white*) growing on 2% glucose. Cells were stained with dihydrorhodamine 123 for 2 h. *C*, flow cytometric analysis of ROS content in W303-1A, u*bp10*Δ, and *ubp10*Δ*sir4*Δ cells growing on 2% glycerol (non-fermentable carbon source). Staining was performed as in *A*.

analysis, we examined the genome-wide transcriptional consequences of deleting *SIR4* in a *ubp10* background to see if *ubp10*Δ*sir4*Δ transcriptional profiles had detectable features that correlated phenotypic and biochemical data (*i.e.* the partial complementation of the growth defect).

Evaluation of the *ubp10 sir4* transcriptional profile revealed that *SIR4* inactivation mitigated the wide transcriptome remodeling of the *ubp10* mutant (see www.ncbi.nlm.nih.gov/geo/). In order to delineate which set of genes was particularly affected in the absence of Sir4p, we initially focused on stress-responsive genes (41–43). Fig. 2*A* shows the fold change values referred to the stress-related genes that were up- and down-regulated in *ubp10*Δ and *ubp10*Δ*sir4*Δ. A clear reduction in the transcriptional response was evident indicating a partial suppression of the stress response induced by loss of *UBP10* alone. No significant change in the transcript level of the same genes was detected in the *sir4* null mutant (data not shown). Fig. 2*A* also reports the fold change values of the stress-responsive genes obtained from the comparison between *ubp10sir4* mutant *versus* the *ubp10* one. It is remarkable that the majority of

these genes falls in the category of down-regulated genes. Thus, the partial complementation of the *ubp10* phenotype following *SIR4* inactivation seems to reflect a reversion of the transcriptional profile detected in the *ubp10* cells. In particular, focusing on the fold change values of a subset of 69 stress-related genes that were all present in the comparisons between *ubp10*/wild type and *ubp10sir4*/*ubp10*, the resulting plot had a symmetrical arrangement with two specular profiles (Fig. 2*B*). A similar plot was obtained for the fold changes values referred to some of the *ubp10* down-regulated genes encoding various transporters, ribosomal proteins, and enzymes for the biosynthesis of amino acids (data not shown), suggesting a recovery of the *ubp10sir4* phenotype strictly linked to a transcriptome remodeling.

Ubp10p has been proposed previously to play a role in Sir4p regulation, and the *ubp10* phenotypic alterations have been suggested to be a consequence of a promiscuous binding of Rap1p-Sir complexes to inappropriate loci leading to a decrease in silencing and transcription of some Rap1p-regulated genes (*i.e.* ribosomal genes). Upon *SIR4* inactivation, the incorrect recruitment of the silencing apparatus and the deleterious gene repression should be prevented (19). Our data are in agreement with this model, supporting an involvement of Ubp10p in transcriptional regulation. In exponentially growing cells, Rap1p targets 294 loci and participates in the activation of 37% of all RNA polymerase II initiation events (55). This fact together with the Rap1p specificity for binding to intergenic sequences potentially acting as promoters (55) could account for the transcription profiling changes detected in the *ubp10* disruptant.

Reduced Silencing Displayed by ubp10 Cells Correlates with an Altered Subtelomeric Gene Expression—Genome-wide technology is a powerful tool for analyzing extensively the transcription of ORFs mapping in subtelomeric chromosomal regions; it allowed us to study the silencing phenomenon without using reporter systems. Referring to the analyses on the *ubp10* single mutant, transcription profiling revealed a predominant effect of reduction in the silencing phenomenon. In detail, we found 24 subtelomeric genes subjected to altered transcription, of which 18 resulted in an increase by a fold change ranging from 2.1 to 10.9, whereas the fold change values of the 6 genes whose expression was reduced were included between −3.5 and −2.3 (Table II). In the double mutant *ubp10sir4,* we detected 54 ORFs whose transcriptional levels changed significantly; 50 appeared more expressed by a fold change ranging from 2.1 to 48.3 and 4 decreased, displaying a fold change between −5.8 and −2.5 (Table III). Rap1p and Sir proteins are required for the silencing of genes located predominantly within 5–10 kb of the ends of the telomeres (56, 57) (Fig. 3*A*). When we examined how the fraction of derepressed subtelomeric genes in the *ubp10* disruptant varied their distance from the chromosome ends, we found *UBP10* deletion up-regulated genes prevalently within 5–10 kb as for the *sir4* mutant, although the global effect of derepression was less pronounced (Fig. 3*A*). Interestingly, in the double disruptant the percentage of up-regulated subtelomeric genes was similar to *sir4* mutant one, but an increase in transcriptional derepression within 15–20 kb of telomeres was observed (Fig. 3*A*) affecting a subtelomeric region where other factors (*i.e.* the histone methyltransferase Set1) play a distinct role from the Sir proteins to maintain silencing (58). Thus, it appears likely that the effects of *UBP10* deletion on subtelomeric silencing are not exclusively mediated by Rap1-Sir complexes.

In addition, Rap-Sir complexes are required for silencing at the *HM* loci. The *MAT* locus codes for three gene regulatory

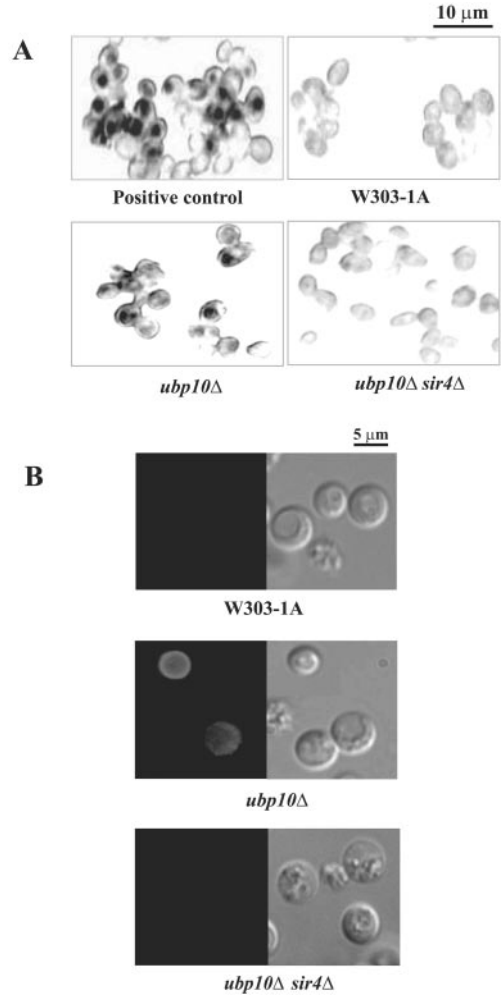

FIG. 5. ***SIR4* inactivation abrogates the *ubp10*Δ apoptotic phenotype.** *A*, DNA strand breakage visualized by the TUNEL reaction-based staining. Positive control was realized by incubating protoplasts with 1 μg/ml DNase I for 20 min at 4 °C (33) before staining. *B*, exposition of phosphatidylserine visualized with FITC-labeled annexin V binding assay (*left side* of each panel). Morphologies of the same cells were visualized by Nomarski (*right side* of each panel). Only protoplasts excluding propidium iodide (and therefore intact) are shown.

proteins that together with a larger group of proteins encoded elsewhere in the genome are responsible for the three distinct types of yeast cells (a, α, and a/α) (59, 60). Consistent with its effect on artificially inserted reporters (19), we found that deletion of *UBP10* in a W303-1A background (*MAT****a***) induced a slight derepression of both *HMRA1* and *HMLALPHA2* genes (Fig. 3*B*), encoding a1 and α2 corepressors, respectively. In the double disruptant, a transcriptional response similar to the one obtained for *sir4*Δ one was present; *HMRA1*, *HMRA2*, as well as *HMLALPHA2* were actively expressed (Fig. 3*B*). Consequently, we observed the related repression of the entire set of a-specific genes (*i.e. MFA1*, *MFA2*, *STE2*, *STE6*, *BAR1,* and *AGA2*) and of some haploid-specific genes, such as *FAR1*, *STE4* and *STE5*. These cells, as expected, were α-factor-resistant (data not shown).

In summary, upon evaluating the global telomeric genes expression in the different strains, the double mutant displayed a more evident derepression effect than *ubp10*, comparable (not identical) to *sir4* single mutant. These results seem to exclude a synergic interaction between *UBP10* and *SIR4* inactivations, but point to an involvement in the same pathway, where Sir4p plays a main role or, alternatively, to parallel pathways with similar targets.

ubp10 Cells Contain ROS in the Absence of External Oxidative Stress—Because the transcriptional stress response was a feature, emerging from the genome-wide analysis of *ubp10*, unrelated to phenotypic traits previously observed, we assayed the sensitivity of *ubp10* cells to different stress conditions (high ethanol, dithiothreitol, UV, high osmolarity, and H_2O_2). A plating assay revealed that mutant cells were more resistant than the wild type to increasing concentrations up to a sub-lethal dose of H_2O_2, suggesting an endogenous tolerance (data not shown). In particular, H_2O_2 tolerance depends on catalase activity, whose gene was up-regulated in the *ubp10* mutant (Table I). Such an endogenous oxidative condition occurs in the cells in the absence of any external oxygen radical sources when ROS, side products of the respiratory metabolism, are no longer detoxified (52, 54). Mitochondrial accumulation of strongly oxidizing molecules is detectable using *in vivo* specific staining reactions depending on the oxidation of fluorochrome precursors. Both *ubp10* and wild type cells in late exponential phase of growth on glucose were incubated with dichlorodihydrofluorescein diacetate for 2 h and then examined under a fluorescence microscope; the mutant population exhibited fluorescent dichlorofluorescein (about 12%), whereas the corresponding wild type cells did not show any signal (Fig. 4*A*). Viability staining with FUN-1 and Calcofluor White M2R revealed that the percentage of fluorescent dichlorofluorescein cells was not due to nonviable cells, and it corresponded to old mother cells (data not shown). The strain background W303 has been reported to harbor the *rad5-535* allele, a weak allele of *RAD5*, which can have additional phenotypic effects when combined with other mutations (61). To rule out the possibility of synergist effects between this allele and *ubp10* null mutation, we inactivated *UBP10* in another strain, BY4741. The disruptants displayed growth defects similar to *ubp10*Δ mutants in the W303 background (data not shown). Moreover, flow cytometric analysis of rhodamine 123 distributions (Fig. 4*B*) showed the presence of cells (about 17%) with high fluorescence in the *ubp10* null mutant (BY4741 background) grown on glucose indicating that ROS accumulation was not strictly correlated to the *rad5* mutation. Thus, the loss of Ubp10 activity triggers ROS accumulation in growth conditions that normally induce no increase of radical production. Finally, ROS presence was tested in cells growing on a non-fermentable carbon source, which imposes respiratory metabolism and consequently forces the mitochondrial activity. Dichlorodihydrofluorescein diacetate was added to *ubp10*, *ubp10sir4,* and wild type cells in late exponential phase of growth on glycerol; after 2 h, samples for each culture were collected and immediately analyzed by flow cytometry. As shown in Fig. 4*C*, the *ubp10* dichlorofluorescein distribution was characterized by a subpopulation of cells (about 25–30%) with high fluorescence, undetectable in the wild type and double mutant strains, in agreement with direct microscopic observation. Similar results have been obtained using dihydrorhodamine 123 (data not shown).

Because the "intensity of respiration" does not induce ROS accumulation (62), the increase in ROS-producing cells suggests that *ubp10* mutants have a leaky mitochondrial electron transport. In fact, ROS generation requires an accumulation of reducing equivalents in the middle portion of the electron transfer chain and then a direct one-electron transfer to a O_2 molecule (63). This diversion of the normal electron flow takes place when the respiratory chain is interrupted, for example by cytochrome *c* release into the cytoplasm. Furthermore, *ubp10sir4* mutant did not accumulate ROS indicating that *SIR4* disruption was sufficient to abrogate this defect.

ubp10 Cells Display Markers of Apoptosis—An increasing amount of evidence supports the occurrence of apoptosis in *S. cerevisiae*, a process in which ROS production has been proposed as a prominent regulatory factor (reviewed in Ref. 64). In fact, ROS accumulate after induction of apoptotic death by various stimuli, such as H_2O_2 and acetic acid (37, 65), in old mother cells (62), in *cdc13-1* mutants (66), and by ectopic expression of BAX, an apoptotic regulator of BCL-2 family (67). In mammalian cells this group of molecules, including both proapoptotic and antiapoptotic proteins, regulates the mitochondria-dependent cell death process, called "intrinsic pathway," by inducing or preventing release of caspases activators, such as cytochrome *c*, from mitochondria to the cytosol (68). To investigate if ROS presence in the *ubp10* disruptant strain was correlated with the apoptotic phenotype, subcellular markers indicating apoptosis were examined. First, we performed the TUNEL assay, a sensitive tool to detect free 3′-OH termini produced by apoptotic DNA cleavage, on *ubp10*, *ubp10sir4,* and wild type cells grown on glycerol. As positive control of the TUNEL reaction, an aliquot of the wild type culture was treated with DNase I to produce DNA fragmentation. As shown in Fig. 5*A*, some *ubp10* cells had an intense staining corresponding to the nucleus, comparable with DNase-treated cells and indicative of DNA strand breakage, whereas the double disruptant and the wild type cells displayed a rarely diffuse staining. In parallel, we carried out on the same cultures an annexin V labeling, in order to detect phosphatidylserine exposure to the external layer of the plasma membrane, another hallmark of apoptosis (69, 70). Simultaneous incubation with FITC-conjugated annexin V and propidium iodide, a membrane-impermeant fluorochrome, revealed a strong fluorescein green fluorescence in some intact *ubp10* cells, whereas all intact spheroplasts of the isogenic control and double mutant showed very slight or no brightness (Fig. 5*B*). Therefore, in addition to ROS accumulation in the mitochondria, *ubp10*Δ mutant displayed a coordinate occurrence of some typical apoptotic features, such as DNA fragmentation and phosphatidylserine exposure, suggesting that loss of the Ubp10 deubiquitinating activity triggers an apoptotic process in an aliquot of the cellular population, which is completely abolished by the lack of Sir4p.

In mammalian cells various substrates of the Ub-dependent proteolytic pathway are involved in the regulation of programmed cell death, but a direct relationship between a deubiquitinating activity and apoptosis was shown only for the tumor suppressor p53. In fact, p53 is a short-lived protein, normally maintained at low level by ubiquitination and consequent proteolysis; deubiquitination by herpes virus-associated ubiquitin-specific protease strongly stabilizes the protein inducing p53-dependent cell growth repression and apoptosis (10). Similarly, the apoptotic phenotype displayed by the *ubp10* mutant could be explained by the final consequence of an unbalanced editing of the ubiquitination state of its substrate(s).

The substrates of Ubp10p are so far unknown, but there is evidence to indicate this enzyme acts in the nucleus and is involved in the network of DNA-proteins interactions affecting silencing and the transcriptional regulation of a large number of genes (Ref. 19 and this work). Changes in chromatin structure are linked not only to the activity of the Rap-Sir complexes but also to histone modifications. In this regard, it is worth recalling that histone mono-ubiquitination does not target the protein to degradation, but it is associated with chromatin remodeling (2, 71, 72). Moreover, in mammalian cells deubiquitination of H2A, coincident with chromatin condensation, occurs in cells undergoing apoptosis as a downstream consequence of caspase activation, but not as a determining apopto-

genic stimulus (73). It is conceivable that in the assembly of a repressed chromatin structure both ubiquitination and deubiquitination of the nucleosomal fibers and of the silencing factors are involved. In the *ubp10* disruptant changes in the equilibrium between ubiquitination and deubiquitination could affect the assembly or the binding activity of regulatory protein(s); this event might alter local chromatin organization and consequently transcription in agreement with the widely detected remodeling of the transcriptome.

Acknowledgments—We thank Caterina Vizzardelli and Monica Capozzoli for technical assistance in microarray analysis and Ettore Virzi for software support. We are also grateful to Giulio Draetta and Hugo Aguilaniu for critical reading of the paper.

REFERENCES

1. Glickman, M. H., and Ciechanover, A. (2002) *Physiol. Rev.* **82,** 373–428
2. Hicke, L. (2001) *Nat. Rev. Mol. Cell. Biol.* **2,** 195–201
3. Hochstrasser, M. (2000) *Nat. Cell Biol.* **2,** 153–157
4. Laney, J. D., and Hochstrasser, M. (1999) *Cell* **97,** 427–430
5. Weissman, A. M. (2001) *Nat. Rev. Mol. Cell. Biol.* **2,** 169–178
6. Ben-Neriah, Y. (2002) *Nat. Immun.* **3,** 20–26
7. Checler, F., da Costa, C. A., Ancolio, K., Chevallier, N., Lopez-Perez, E., and Marambaud, P. (2000) *Biochim. Biophys. Acta* **1502,** 133–138
8. Schwartz, A. L., and Ciechanover, A. (1999) *Annu. Rev. Med.* **50,** 57–74
9. Chung, C. H., and Baek, S. H. (1999) *Biochem. Biophys. Res. Commun.* **266,** 633–640
10. Li, M., Chen, D., Shiloh, A., Luo, J., Nikolaev, A. Y., Qin, J., and Gu, W. (2002) *Nature* **416,** 648–653
11. Wilkinson, K. D. (2000) *Semin. Cell Dev. Biol.* **11,** 141–148
12. Amerik, A. Y., Li, S.-J., and Hochstrasser, M. (2000) *Biol. Chem. Hoppe-Seyler* **381,** 981–992
13. Amerik, A. Y., Swaminathan, S., Krantz, B. A., Wilkinson, K. D., and Hochstrasser, M. (1997) *EMBO J.* **16,** 4826–4838
14. Papa, F., and Hochstrasser, M. (1993) *Nature* **366,** 313–319
15. Amerik, A. Y., Nowak, J., Swaminathan, S., and Hochstrasser, M. (2000) *Mol. Biol. Cell* **11,** 3365–3380
16. Papa, F. R., Amerik, A. Y., and Hochstrasser, M. (1999) *Mol. Biol. Cell* **10,** 741–756
17. Swaminathan, S., Amerik, A. Y., and Hochstrasser, M. (1999) *Mol. Biol. Cell* **10,** 2583–2594
18. Singer, M. S., Kahana, A., Wolf, A. J., Meisinger, L. L., Peterson, S. E., Goggin, C., Mahowald, M., and Gottschling, D. E. (1998) *Genetics* **150,** 613–632
19. Kahana, A., and Gottschling, D. E. (1999) *Mol. Cell. Biol.* **19,** 6608–6620
20. Gasser, S. M., and Cockell, M. M. (2001) *Gene* (*Amst.*) **279,** 1–16
21. Huang, Y. (2002) *Nucleic Acids Res.* **30,** 1465–1482
22. Denu, J. M. (2003) *Trends Biochem. Sci.* **28,** 41–48
23. Gotta, M., Laroche, T., Formenton, A., Maillet, L., Scherthan, H., and Gasser, S. M. (1996) *J. Cell Biol.* **134,** 1349–1363
24. Smith, J. S., and Boeke, J. D. (1997) *Genes Dev.* **11,** 241–254
25. Smith, J. S., Brachmann, C. B., Pillus, L., and Boeke, J. D. (1998) *Genetics* **149,** 1205–1219
26. Chang, J.-F., Hall, B. E., Tanny, J. C., Moazed, D., Filman, D., and Ellenberger, T. (2003) *Structure* **11,** 637–649
27. Luo, K., Vega-Palas, M. A., and Grunstein, M. (2002) *Genes Dev.* **16,** 1528–1539
28. Moazed, D., and Johnson, D. (1996) *Cell* **86,** 667–677
29. Kahana, A. (2001) *Biochem. Biophys. Res. Commun.* **282,** 916–920
30. Rothstein, R. J. (1983) *Methods Enzymol.* **101,** 202–211
31. Vanoni, M., Vai, M., Popolo, L., and Alberghina, L. (1983) *J. Bacteriol.* **156,** 1282–1291
32. Hill, J., Ian, K. A., Donald, G., and Griffiths, D. E. (1991) *Nucleic Acids Res.* **19,** 5791
33. Sambrook, J., Fritsch, E. F., and Maniatis, T. (1989) *Molecular Cloning: A Laboratory Manual*, 2nd Ed., Cold Spring Harbor Laboratory Press, Cold Spring Harbor, NY
34. Federoff, H. J., Cohen, J. D., Eccleshall, T. L., Needleman, R. B., Buchferer, B. A., Giacalone, J., and Marmur, J. (1982) *J. Bacteriol.* **149,** 1064–1070
35. Granucci, F., Vizzardelli, C., Pavelka, N., Feau, S., Persico, M., Virzi, E., Rescigno, M., Moro, G., and Ricciardi-Castagnoli, P. (2001) *Nat. Immun.* **2,** 882–888
36. Popolo, L., Cavadini, P., Vai, M., and Alberghina, L. (1993) *Curr. Genet.* **24,** 382–387
37. Madeo, F., Fröhlic, E., Ligr, M., Grey, M., Sigrist, S. J., Wolf, D. H., and Fröhlic, K.-U. (1999) *J. Cell Biol.* **145,** 757–767
38. Ligr, M., Velten, I., Fröhlic, E., Madeo, F., Ledig, M., Fröhlic, K.-U., Wolf, D. H., and Hilt, W. (2001) *Mol. Biol. Cell* **12,** 2422–2432
39. Kennedy, B. K., Austriaco, N. R., Jr., Zhang, J., and Guarente, L. (1995) *Cell* **80,** 485–496
40. ter Linde, J. J., Liang, H., Davis, R. W., Steensma, H. Y., van Dijken, J. P., and Pronk, J. T. (1999) *J. Bacteriol.* **181,** 7409–7413
41. Causton, H. C., Ren, B., Koh, S. S., Harbison, C. T., Kanin, E., Jennings, E. G., Lee, T. I., True, H. L., Lander, E. S., and Young, R. A. (2001) *Mol. Biol. Cell* **12,** 323–337
42. Gasch, A. P., Spellman, P. T., Kao, C. M., Carmel-Harel, O., Eisen, M. B., Storz, G., Botstein, D., and Brown, P. O. (2000) *Mol. Biol. Cell* **11,** 4241–4257
43. Rep, M., Krantz, M., Thevelein, J. M., and Hohmann, S. (2000) *J. Biol. Chem.* **275,** 8290–8300
44. Moskvina, E., Shüller, C., Maurer, C. T. C., Mager, W. H., and Ruis, H. (1998) *Yeast* **14,** 1041–1050
45. Posas, F., Chambers, J. R., Heyman, J. A., Hoeffler, J. P., de Nada, E., and Ariño, J. (2000) *J. Biol. Chem.* **275,** 17249–17255
46. Yale, J., and Bohnert, H. J. (2001) *J. Biol. Chem.* **276,** 15996–16007
47. Cheng, L., Watt, R., and Piper, P. W. (1994) *Mol. Gen. Genet.* **243,** 358–362
48. Baba, M., Osumi, M., Scott, S. V., Klionsky, D. J., and Ohsumi, Y. (1997) *J. Cell Biol.* **139,** 1687–1695
49. Godon, C., Lagniel, G., Lee, J., Buhler, J. M., Kieffer, S., Perrot, M., Boucherie, H., Toledano, M. B., and Labarre, J. (1998) *J. Biol. Chem.* **273,** 22480–22489
50. Higgins, V. J., Alic, N., Thorpe, G. W., Breitenbach, M., Larsson, V., and Dawes, I. W. (2002) *Yeast* **19,** 203–214
51. Groot Koerkamp, M., Rep, M., Bussemaker, H. G., Hardy, G. P. M. A., Mul, A., Piekarska, K., Al-Khalili Szigyarto, C., Teixeira de Mattos, J. M., and Tabak, H. F. (2002) *Mol. Biol. Cell* **13,** 2783–2794
52. Jamieson, D. J. (1998) *Yeast* **14,** 1511–1527
53. Collinson, E. J., Wheeler, G. L., Ocón Garrido, E., Avery, A. M., Avery, S. V., and Grant, C. M. (2002) *J. Biol. Chem.* **277,** 16712–16717
54. Estruch, F. (2000) *FEMS Microbiol. Rev.* **24,** 469–486
55. Lieb, D. J., Liu, X., Botstein, D., and Brown, P. O. (2001) *Nat. Genet.* **28,** 327–334
56. Hughes, T. R., Marton, M. J., Jones, A. R., Roberts, C. J., Stoughton, R., Armour, C. D., Bennett, H. A., Coffey, E., Dai, H., He, Y. D., Kidd, M. J., King, A. M., Meyer, M. R., Slade, D., Lum, P. Y., Stepaniants, S. B., Chakraburtty, K., Simon, J., Bard, M., and Friend, S. H. (2000) *Cell* **102,** 109–126
57. Wyrick, J. J., Holstege, F. C. P., Jennings, E. G., Causton, H. C., Shore, D., Grunstein, M., Lander, E. S., and Young, R. A. (1999) *Nature* **402,** 418–421
58. Bernstein, B. E., and Schreiber, S. L. (2002) *Chem. Biol.* **9,** 1167–1173
59. Gelli, A. (2002) *Mol. Microbiol.* **46,** 845–854
60. Johnson, A. D. (1995) *Curr. Opin. Genet. Dev.* **5,** 552–558
61. Fan, H.-Y., Cheng, K. K., and Klein, H. L. (1996) *Genetics* **142,** 749–759
62. Laun, P., Pichova, A., Madeo, F., Fuchs, J., Ellinger, A., Sepp, K., Dawes, I., Fröhlic, K.-U., and Breitenbach, M. (2001) *Mol. Microbiol.* **39,** 1166–1173
63. Cai, J., and Jones, D. P. (1998) *J. Biol. Chem.* **273,** 11401–11404
64. Madeo, F., Engelhardt, S., Herker, E., Lehmann, N., Maldener, C., Proksch, A., Wissing, S., and Fröhlic, K.-U. (2002) *Curr. Genet.* **41,** 208–216
65. Ludovico, P., João Sousa, M., Silva, M. T., Leão, C., and Côrte Real, M. (2001) *Microbiology* **147,** 2409–2415
66. Qi, H., Li, T.-K., Kuo, D., Nur-E-Kamal, A., and Liu, L. F. (2003) *J. Biol. Chem.* **278,** 15136–15141
67. Gross, A., Pilcher, K., Blachly-Dyson, E., Basso, E., Jockel, J., Bassik, M. C., Korsmeyer, S. J., and Forte, M. (2000) *Mol. Cell. Biol.* **20,** 3125–3136
68. Matsuyama, S., Llopis, J., Deveraux, Q. L., Tsien, R. Y., and Reed, J. C. (2000) *Nat. Cell Biol.* **2,** 318–325
69. Fröhlic, K.-U., and Madeo, F. (2000) *FEBS Lett.* **473,** 6–9
70. Madeo, F., Fröhlic, E., and Fröhlic, K.-U. (1997) *J. Cell Biol.* **139,** 729–734
71. Briggs, S. D., Xiao, T., Sun, Z.-W., Caldwell, J. A., Shabanowitz, J., Hunt, D. F., Allis, C. D., and Strahl, B. D. (2002) *Nature* **418,** 498
72. Sun, Z.-W., and Allis, D. (2002) *Nature* **418,** 104–108
73. Mimnaugh, E. G., Kayastha, N. B., McGovern, N. B., Hwang, S.-G., Marcu, M. G., Trepel, J., Cai, S.-Y., Marchesi, V. T., and Neckers, L. (2001) *Cell Death Differ.* **8,** 1182–1196

Transcriptional Profiling of *ubp10* Null Mutant Reveals Altered Subtelomeric Gene Expression and Insurgence of Oxidative Stress Response

Ivan Orlandi, Maurizio Bettiga, Lilia Alberghina and Marina Vai

J. Biol. Chem. 2004, 279:6414-6425.
doi: 10.1074/jbc.M306464200 originally published online November 17, 2003
